



HAL
open science

Sucrose and Glycerol Additives: A Way to Tune the Biological and Physicochemical Properties of Agarose Hydrogels?

Victor C Igbokwe, Vincent Ball, Nour-ouda Benzaamia, Simon Gree, Sophie Hellé, Juliette Soubirou-blot, Corinne Nardin, Lydie Ploux

► **To cite this version:**

Victor C Igbokwe, Vincent Ball, Nour-ouda Benzaamia, Simon Gree, Sophie Hellé, et al.. Sucrose and Glycerol Additives: A Way to Tune the Biological and Physicochemical Properties of Agarose Hydrogels?. *Macromolecular Materials and Engineering*, 2024, 10.1002/mame.202400150 . hal-04647850

HAL Id: hal-04647850

<https://univ-pau.hal.science/hal-04647850>

Submitted on 15 Jul 2024

HAL is a multi-disciplinary open access archive for the deposit and dissemination of scientific research documents, whether they are published or not. The documents may come from teaching and research institutions in France or abroad, or from public or private research centers.

L'archive ouverte pluridisciplinaire **HAL**, est destinée au dépôt et à la diffusion de documents scientifiques de niveau recherche, publiés ou non, émanant des établissements d'enseignement et de recherche français ou étrangers, des laboratoires publics ou privés.



Distributed under a Creative Commons Attribution 4.0 International License

Sucrose and Glycerol Additives: A Way to Tune the Biological and Physicochemical Properties of Agarose Hydrogels?

Victor C. Igbokwe, Vincent Ball, Nour-Ouda Benzaamia, Simon Gree, Sophie Hellé, Juliette Soubirou-Blot, Corinne Nardin,* and Lydie Ploux*

Sucrose and glycerol have gained attention as additives for hydrogels, owing to their capacity to exert considerable influence over the physicochemical, mechanical, and biological characteristics of these materials. Herein, these effects on agarose hydrogels (AHs) are explored. A series of AHs are synthesized using sucrose (30% and 300% w/v) and glycerol as additives. The storage modulus (10.0–13.7 kPa) and hydrophilicity of the hydrogels (contact angle < 50°) do not vary significantly with sucrose or glycerol addition. However, sucrose enhances the hydration capacity of the hydrogels by up to 170%, whereas glycerol reduces it. Interestingly, sucrose and glycerol individually do not have bacteriostatic effects against *Staphylococcus epidermidis*, but their combination significantly ($p \leq 0.001$) inhibits the growth of both *S. epidermidis* and *Pseudomonas aeruginosa* by 63% and 29%, respectively, in comparison to native agarose. Cytotoxicity testing on NIH/3T3 murine fibroblasts reveals that sucrose increases cell viability up to 98%, while glycerol reduces it below 60%. Overall, these hydrogels hold promise for antibacterial biomedical applications as wound dressing materials and surface coatings for medical devices and can also be used to formulate bioinks for 3D bioprinting.

applications. These applications include tissue engineering, drug delivery, 3D bioprinting, and biosensing.^[1–4] Additionally, hydrogels have been employed to coat both biotic and abiotic surfaces, such as wounds and medical devices respectively.^[5,6] Hydrogels derived from natural polymers have garnered substantial interest due to their renewability, biodegradability, compatibility with living cells and tissues, and the relative ease of functional modification have rendered them indispensable.^[7–9] Among the diverse spectrum of natural polymers used to synthesize hydrogels, agarose stands out prominently. This prominence can be attributed to its thermo-reversible gelation behavior, ease of modification, water solubility, and tunable mechanical properties.^[10–12] Furthermore, agarose is generally regarded as biocompatible and exhibits a striking resemblance to the extracellular matrix, making it a suitable candidate for various biomedical applications, particularly in tissue engineering and regenerative medicine.^[12] Notably, agarose is also biodegradable and hypoallergenic.^[13]

Agarose is a neutral hydrophilic biopolymer sourced from seaweed. It comprises 400 agarobiose repeating units, composed of 1,3-linked-d-galactopyranose and 1,4-linked 3,6-anhydro- α -

1. Introduction

Hydrogels have revolutionized the design and development of innovative functional biomaterials for various biomedical

V. C. Igbokwe, V. Ball, N.-O. Benzaamia, S. Hellé, L. Ploux
INSERM
UMR-S 1121 Biomaterial Bioengineering
Centre de Recherche en Biomédecine de Strasbourg
Strasbourg 67000, France
E-mail: ploux@unistra.fr

V. C. Igbokwe, V. Ball, N.-O. Benzaamia, S. Hellé, L. Ploux
Faculty of Dentistry
Université de Strasbourg
Strasbourg 67000, France

V. C. Igbokwe, V. Ball, N.-O. Benzaamia, S. Hellé, L. Ploux
CNRS
EMR 7003, Strasbourg 67000, France

S. Gree
CNRS
UMR 7361 IS2M
Université de Haute-Alsace
Mulhouse 68200, France

J. Soubirou-Blot, C. Nardin
E2S UPPA
CNRS
IPREM
Université de Pau et des Pays de l'Adour
Pau 64000, France
E-mail: corinne.nardin@univ-pau.fr

 The ORCID identification number(s) for the author(s) of this article can be found under <https://doi.org/10.1002/mame.202400150>

© 2024 The Author(s). Macromolecular Materials and Engineering published by Wiley-VCH GmbH. This is an open access article under the terms of the [Creative Commons Attribution](https://creativecommons.org/licenses/by/4.0/) License, which permits use, distribution and reproduction in any medium, provided the original work is properly cited.

DOI: 10.1002/mame.202400150

l-galactopyranose.^[14,15] This chemical structure incorporates several polar functional groups and linkages, including —OH, —O—, and C=O, conferring it with a strong hydrophilic property and the ability to form hydrogen bonds with water molecules. This property is pivotal in the context of hydrogel formation.^[10] Agarose hydrogels (AHs) can be easily formulated under simple conditions without the need for catalysts, unlike hydrogels synthesized with other biopolymers such as cellulose and guar gum.^[16] While native AHs have their advantages, they are inherently biologically inert and lack intrinsic antibacterial properties. This limits their applicability in antibacterial contexts, and their high water content may make them susceptible to bacterial proliferation.^[17] Given that bacteriostatic or bactericidal properties are highly desirable in biomaterials for biomedical applications,^[18] various studies have focused on developing antibacterial AHs through chemical modification or the incorporation of antibacterial agents, such as classical antibiotics, nanoparticles, and polyphenols.^[19–23] However, the use of these antibacterial agents often presents significant challenges, including issues related to antibiotic resistance,^[24–26] cytotoxicity,^[27,28] environmental concerns,^[29] relatively high cost of production,^[30] and in some cases, limited spectrum of efficacy.^[27] Considering these challenges, we explored the feasibility of using a combination of sucrose and glycerol to synthesize antibiotics-free bacteriostatic AHs.

Sucrose, glycerol, and their derivatives are widely recognized as safe additives in the fields of food and pharmaceuticals,^[31–33] prompting their extensive use. In the context of biomedical applications, they have garnered substantial interest for their capacity to modify the physicochemical, mechanical, and biological properties of hydrogels. Specifically, sucrose can enhance the affinity of agarose polymer helices for solvents, thereby limiting helix aggregation tendencies and influencing the mechanical properties of agarose gels.^[34] Historically, sugars have also been used in wound healing for centuries probably due to their antibacterial activity.^[35] Additionally, both sucrose and its derivatives exhibit antibacterial properties at high concentrations.^[36–38] However, sucrose at low concentration can be metabolized by many microorganisms and used as a carbon source,^[39] thus possibly facilitating microbial growth. On the other hand, glycerol has been noted for its capacity to enhance the flexibility and softness of agarose gels by improving the mobility of polymer chains under deformation.^[13] Like sucrose, glycerol and its derivatives have also shown interesting antibacterial activities.^[32,40] Though specific figures on the cost and availability of sucrose and glycerol vary with factors such as location, supplier, and quantity required, the consistent use of sucrose and glycerol in various industrial and research applications strongly suggests that they are relatively inexpensive and readily accessible.

In this study, we investigated the possibility of combining sucrose and glycerol as additives to impart antibacterial properties to AHs intended for biomedical applications. To achieve this, we synthesized two series of AHs using glycerol and varied concentrations of sucrose. The concentration of glycerol used was fixed at the lower threshold of the optimal range (from 30% to 50% of the material weight) required to have a plasticizing effect, while limiting the risk of toxicity.^[41] The concentration of sucrose used in this study was well below the levels (30–60% of the material weight) used in food preservation.^[42] The selected concentration

Table 1. Hydrogel composition in terms of the weight of compounds used for hydrogel formulation.

	Sample ID	Agarose [g]	Sucrose [g]	Glycerol [g]
A-series	A1	0.15	–	–
	AG	0.15	–	6.31
	AS ₃₀	0.15	0.05	–
	AGS ₃₀	0.15	0.05	6.31
	AS ₃₀₀	0.15	0.45	–
	AGS ₃₀₀	0.15	0.45	6.31
B-series	B1	0.30	–	–
	BG	0.30	–	6.31
	BS ₃₀	0.30	0.09	–
	BGS ₃₀	0.30	0.09	6.31
	BS ₃₀₀	0.30	0.90	–
	BGS ₃₀₀	0.30	0.90	6.31

is expected to release a minimal quantity of sucrose, thus limiting possible inflammatory drawbacks. Our experimental approach involved synthesizing two different series of hydrogels—A-series and B-series. The concentration of agarose in the B-series hydrogels was twice that of the A-series. However, it is important to note that the ratio of agarose to sucrose and agarose to glycerol remained constant within each hydrogel within each series. The primary objectives of this study were to evaluate the effect of the additives on the i) surface wettability and hydration capacity, ii) dynamic viscoelasticity, iii) bacteriostatic activity against *Staphylococcus epidermidis* and *Pseudomonas aeruginosa*, and iv) biocompatibility of AHs. The effect of the additives on the surface chemistry and the possible release of compounds from the hydrogels was evaluated as well.

2. Experimental Section

2.1. Materials

Agarose (CAS No. 9012-36-6) was purchased as a fine white powder from Sigma–Aldrich (Darmstadt, Germany) with a specific gelling temperature (T_{gel}) between 34.5 and 37.5 °C and a gel strength of >1200 g cm⁻² as stated by the producer. Analytical grade (99% pure) glycerol (CAS No. 56-81-5) having a boiling point of 180 °C and molecular weight of 92.09 g mol⁻¹ was purchased from Fisher Scientific GmbH (Kehl, Germany). Food grade, for human consumption sucre+ (Cestas, France) E+ organic beet sugar was purchased from Biocoop (Strasbourg, France). For the bacteriostatic activity assays, trypticasein soy broth and agar agar from Condalab (Madrid, Spain) and BD Bacto (New Jersey, USA) respectively were used. All reagents and materials were used without further purification or modification.

2.2. Synthesis of Hydrogels

Two sets of hydrogels (A-series and B-series) were synthesized in one-pot by varying the concentration of sucrose at 30% and 300% (w/v), while maintaining the concentration of glycerol as shown in **Table 1**. Notably, the respective concentration of agarose and sucrose in the B-series samples was consistently twice that

of the A-series. Agarose, sucrose, and glycerol were concurrently added into a glass vessel and mixed with 15 mL of freshly prepared saline (NaCl solution, 0.9% w/v) to be in physiological-like conditions. Afterward, the glass vessel was closed with a lid and heated at 90 ± 10 °C for 25 min under stirring at 400 rpm. The resulting clear solution was cast into a 90×15 mm polystyrene Petri dish, which was left half-open to prevent steam accumulation on the hydrogel surface during gelation. After at least 20 min of setting at room temperature, the hydrogel samples were cut into 14 mm discs using a hollow punch (Boehm SAS, La Fouillouse, France). The 14 mm diameter cut of the hydrogel samples was used for all physicochemical and antibacterial characterizations unless otherwise stated.

2.3. Characterization of the Hydrogels

2.3.1. Surface Wettability

The surface wettability of the hydrogels was determined by contact angle (CA) measurement in the sessile drop mode at room temperature using an Attension Theta goniometer (Biolin Scientific, Västra Frölunda, Sweden). Using an automated micropipette, a drop (5 μ L) of Milli-Q water was carefully deposited via a 0.7 mm inner diameter tip at different randomly selected locations on the surface of the hydrogel. An image per 0.07 s was recorded by a CCD camera connected to the device from the moment the drop of water hit the surface of the hydrogel until it reached a stable shape. The images were acquired, and the CA was determined after numerical fitting of the droplet shape based on the Young–Laplace model.^[43] At least five measurements were taken per two independent replicates of each sample, and the data obtained were presented as mean \pm SD. Based on the CA values, the surfaces of the hydrogels were classified as hydrophobic (when CA > 90°) or hydrophilic (when CA < 90°).^[44]

2.3.2. Hydration Capacity

The hydration capacity (HC) of the hydrogels in physiological serum was determined by mass measurement. Briefly, 14 mm samples of the hydrogels, with an average thickness between 2 and 3 mm were dried to a constant weight in an incubator at 37 °C. The weight of the samples after achieving equilibrium weight was recorded as the initial weight (W_1). Subsequently, the samples were placed in a 12-well plate and submerged in 0.9% NaCl solution at room temperature. The microplate was covered to minimize evaporation. The weight of the samples was monitored until they attained equilibrium, and the weight was recorded as W_2 . The HC of the hydrogels was calculated using Equation 1 and expressed as mean \pm SD of at least six independent replicates of each sample.

$$\text{HC (\%)} = \frac{W_2 - W_1}{W_1} \times 100 \quad (1)$$

where W_1 is the weight of the hydrogel after dehydration at 37 °C while W_2 is the weight of the hydrogel at equilibrium of swelling in 0.9% NaCl solution at room temperature.

2.3.3. Dynamic Viscoelasticity

The dynamic storage (G') and loss (G'') modulus of the preformed hydrogels were determined at a frequency range of 30.00 to 0.01 Hz using a Malvern Kinexus Ultra+ rheometer in a plate-plate configuration. The diameter of the upper geometry was 20 mm. A gap of between 1.8 to 2.5 mm between the upper and lower plates was set, representing $\approx 90\%$ of the sample thickness. Rheology measurement was done with a compression deformation of between 0.2 and 0.3% (10% based on the sample thickness) and constant temperature of 25 °C. G' and G'' values were reported as mean \pm SD of three independent replicates per sample.

2.3.4. Surface Chemistry

Raman spectra of the hydrogels were acquired at two distinct locations: at the surface and at a depth of 500 μ m. Hydrogel samples of 14 mm diameter were placed on a silicon wafer substrate and the Raman spectra were acquired using a PerkinElmer spectrometer equipped with a 532 nm laser for excitation. Spectra were acquired in the confocal mode and afterwards processed with Spectragryph v1.2.16.1. The characteristic peaks were identified and assigned according to the literature.

2.3.5. Sucrose and Glycerol Release

The quantity of sucrose and glycerol released from the hydrogels in water respectively was estimated by Fourier transformed infrared spectroscopy (FTIR). A 14 mm diameter cut of the hydrogel samples was placed in Eppendorf tubes and submerged with 2 mL of milli-Q water for 24 h at room temperature. Afterward, the hydrogels were recovered from the Eppendorf tubes, and the supernatant was deposited over the attenuated total reflection (ATR) accessory after mixing properly. For an enhanced sensitivity, all spectra were obtained with an MCT detector between 650 and 4000 cm^{-1} with a resolution of 4 cm^{-1} . The spectrum of milli-Q water on the ATR accessory measured at room temperature was used as the background. The ATR-infrared spectra were recorded as absorbance. The peak heights at 1044 cm^{-1} for glycerol and 1056 cm^{-1} for sucrose which corresponds to the stretching vibration of C-O in glycerol^[45,46] and sucrose,^[47–49] respectively were utilized as the characteristic peaks of sucrose and glycerol for the estimation of their respective concentrations in the supernatants comparison. The heights were compared to absorbance-concentration calibration curves for glycerol and sucrose (Figure S1a,b, Supporting Information), which were established using their pure solutions with known concentrations, thus enabling the estimation of released amounts.

2.3.6. Bacterial Growth Inhibition

The inhibitory effect of the hydrogels on the growth of the test organisms, *Pseudomonas aeruginosa* ATCC 27853 and *Staphylococcus epidermidis* ATCC 35984, in planktonic state was evaluated by optical density measurement at 600 nm (OD_{600}). A 14 mm

sample of the respective hydrogels was carefully placed into a 12-well microplate. Subsequently, the samples were inoculated with a 2 mL suspension of *P. aeruginosa* and *S. epidermidis*, respectively, preculture grown overnight in tryptic soy broth (TSB) at 37 °C in an incubator shaker. An inoculum of each test organism without any supplementary material or substance was used as a control. The samples inoculated with the test organisms were then incubated at 37 °C for 24 h in a static incubator, following which the OD₆₀₀ of the suspension was measured by a Bio-Rad SmartSpec Plus spectrophotometer, with TSB as the blank. The OD₆₀₀ values of the test organisms were converted to Log colony forming units per mL (Log CFU mL⁻¹) using an OD-CFU mL⁻¹ standard curve for the respective test organisms. The experiments were replicated a minimum of three times on at least three independent samples, thereby resulting in a total of at least nine replicates per hydrogel sample.

2.3.7. In Vitro Cytotoxicity

The cytotoxicity of the hydrogels was assessed by quantifying the viability of a NIH/3T3 mouse fibroblast cells on hydrogel extracts using 3-(4,5-dimethylthiazol-2-yl)-2,5-diphenyltetrazolium bromide (MTT) in accordance with the ISO-10993-5 protocol,^[50] with some modifications. Hydrogel samples, cut into 12 mm diameter circles using a sterile biopsy punch, were carefully placed in a 24-well microplate, and sterilized with UV light for 15 min before extraction. To prepare hydrogel extracts, 1 mL of high-glucose Dulbecco's modified Eagle medium (DMEM, Dutscher France) was dispensed into the wells containing the hydrogel samples and subsequently incubated for 24 h at 37 °C. Besides, fibroblasts previously cultured in DMEM supplemented with 10% fetal bovine serum (FBS) and 1% antibiotics (penicillin and streptomycin), for 24 h at 37 °C in a 5% CO₂ atmosphere, were diluted with complete DMEM to achieve a final concentration of 5 × 10⁴ cells mL⁻¹. 200 μL of this cell suspension was seeded into wells of a 24-well microplate and incubated for 24 h. The medium was then replaced by the hydrogel extracts and incubated for 24 h. Complete DMEM and dimethyl sulfoxide (DMSO) were used as positive and negative controls, respectively. Following incubation, the supernatants were discarded while the cells attached to the wall of the microplate were washed with phosphate buffer saline (PBS). 100 μL of 0.5 mg mL⁻¹ MTT solution in DMEM was added into each well and incubated for a minimum of 2 h. After discarding the solution, 100 μL of DMSO was added to the wells to dissolve the purple formazan crystals formed. The resulting solution's absorbance was measured at 570 nm using a spectrophotometer. Cell viability was calculated using Equation 2 and reported as mean ± SD of three replicates per at least three independent samples per hydrogel.

$$\text{Cell viability (\%)} = \frac{\text{Mean absorbance of hydrogel samples}}{\text{Mean absorbance of positive control (DMEM)}} \times 100 \quad (2)$$

2.4. Statistical Analysis

All data are presented as mean ± SD. To test for statistical significance of the difference between the means of the treatments

Table 2. Concentration in every compound related to the weight of the final hydrogel.

	Sample ID	Agarose [% w/w [§]]	Sucrose [% w/w [§]]	Glycerol [% w/w [§]]
A-series	A1	1.3 ± 0.1	–	–
	AG	0.8 ± 0.1	–	34.7 ± 1.6
	AS ₃₀	1.4 ± 0.2	0.5 ± 0.1	–
	AGS ₃₀	0.8 ± 0.1	0.3 ± 0.1	34.7 ± 1.6
	AS ₃₀₀	1.2 ± 0.1	3.6 ± 0.1	–
	AGS ₃₀₀	0.8 ± 0.1	2.3 ± 0.1	32.5 ± 2.1
B-series	B1	2.7 ± 0.1	–	–
	BG	1.6 ± 0.1	–	34.7 ± 0.8
	BS ₃₀	2.8 ± 0.3	0.8 ± 0.1	–
	BGS ₃₀	1.7 ± 0.1	0.5 ± 0.1	35.5 ± 1.7
	BS ₃₀₀	2.6 ± 0.1	7.8 ± 0.3	–
	BGS ₃₀₀	1.6 ± 0.1	4.8 ± 0.3	33.9 ± 2.3

§: referred to the weight of the material as obtained after synthesis and following stabilization of the hydration state at the room condition.

and control (A1), the normality of the data was first determined using the Shapiro–Wilk test. If the means followed a normal distribution, the Tukey post-hoc test was used to analyze the difference. However, if the means were not normally distributed, the Kruskal–Wallis's test and the Dunn's multiple comparison to analyze the difference. *, **, and *** were used to label means that were significantly different from the control at $p \leq 0.05$, 0.01 and 0.001 respectively.

3. Results and Discussion

Two series of AHs were synthesized. The weight/weight concentration of agarose, sucrose, and glycerol relative to the final hydrogel (considered after formulation and stabilization for about 20 min under ambient conditions) are presented in **Table 2**. The concentration of agarose in the B-series of hydrogels is twice that of the A-series. The concentration of glycerol was ≈34% for all the samples, just higher than the limit allowing glycerol to play its plasticizer role.^[41] The concentration of sucrose varied from 0.3 to 7.8%, thus largely lower than the limits of concentration for a preservation effect.

3.1. Surface Wettability

The surfaces of the hydrogels exhibited pronounced wettability (**Figure 1**), with CA values between 35° and 42°, which is typical of hydrophilic surfaces.^[44] Also, increasing the concentration of agarose decreased the CA of all the hydrogels (**Figure S2**, Supporting Information), whatever the concentration in the other compounds. This suggests that agarose had a predominant influence on the wettability of the surface of the hydrogels. This surface hydrophilicity of the hydrogels was not surprising since sucrose and agarose have abundant polar chemical groups like OH in their respective chemical structures.^[51]

In contrast, sucrose did not affect the CA of the hydrogels. As seen with AS30 and AS300, there was no significant difference

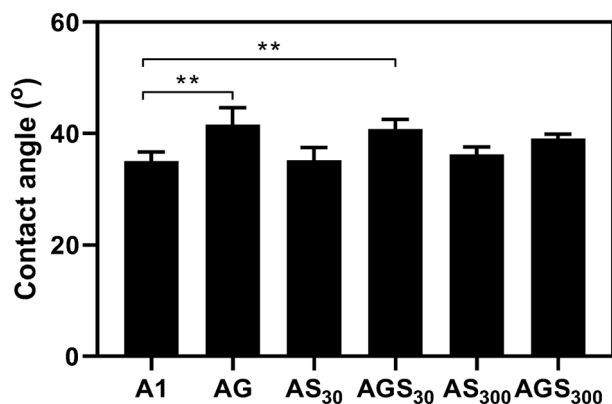


Figure 1. Surface wettability of the series A of hydrogels (presented as mean \pm SD, $n \geq 4$).

in the CA of the hydrogels compared to the native agarose (A1), irrespective of the concentration of sucrose. There was also no significant difference in the CA of AGS30 and AGS300 compared to AG.

Glycerol also did not affect the CA in the B-series irrespective of the sucrose concentration. However, glycerol slightly increased the CA in the A-series as seen with AG and AGS30. This suggests that the influence of glycerol on the surface wettability of the hydrogels was significant only for glycerol-to-agarose ratio much higher than 20. Meanwhile, the increase in CA due to glycerol was surprising given that glycerol is a polar and hydrophilic molecule.^[52] One possible explanation for this unexpected result is that glycerol diffused from the hydrogel's matrix to the surface during gelation. This diffusion may have created a thin, viscous layer on the hydrogel's surface, increasing its roughness (Figure S3, Supporting Information) and consequently increasing its CA.

3.2. Hydration Capacity

The maximum swelling of the hydrogels in a physiological saline solution was used as an index of their hydration capacity (HC). We observed a systematic pattern in the HC, as illustrated in Figure 2a and Figure S4a (Supporting Information) for series A and B, respectively. The HC of A1 was 150%, whereas agarose hydrogels containing glycerol had a reduced HC compared to A1, with AG, AGS₃₀, and AGS₃₀₀ exhibiting HCs of 21%, 25%, and 19%, respectively. This behavior was also consistent in the B-series hydrogels. Glycerol thus strongly affected the hydration capacity of the hydrogels.

Notably, as depicted in Figure 2b,c, glycerol prominently affected the rate of dehydration and rehydration in comparison to A1 and the hydrogels containing only sucrose. Specifically, while the mean hydration rate of AS₃₀ ($5.2 \times 10^{-2} \text{ g h}^{-1}$) and AS₃₀₀ ($5.1 \times 10^{-2} \text{ g h}^{-1}$) did not differ from that of A1 ($5.1 \times 10^{-2} \text{ g h}^{-1}$), those of AG ($1.8 \times 10^{-2} \text{ g h}^{-1}$), AGS₃₀ ($1.9 \times 10^{-2} \text{ g h}^{-1}$), and AGS₃₀₀ ($1.9 \times 10^{-2} \text{ g h}^{-1}$) were 2.79, 2.66, and 2.66 times lower. Glycerol did also retard the mean rate of dehydration by approximately 1.5, with a dehydration rate of $4.0 \times 10^{-2} \text{ g h}^{-1}$, for A1, AS₃₀, and AS₃₀₀, but 2.7×10^{-2} , 2.8×10^{-2} , and $2.6 \times 10^{-2} \text{ g h}^{-1}$ for AG, AGS₃₀, and AGS₃₀₀, respectively. This may be due to a substantial quantity of fluids trapped within the hydrogel matrix which were probably

not expelled during dehydration, prior to immersion in saline. Balik-Was et al.^[53] and Xu et al.^[54] reported similar observations, attributing this phenomenon to the strong hydrogen bonding interactions between glycerol and water,^[45,55,56] as well as the low volatility and high boiling point of glycerol.^[57]

A supplementary explanation for the anti-hydration effect of glycerol is its potential role as a potent plasticizer,^[58,59] which reduced the crosslink density of the agarose polymer chains within the hydrogel matrix, effectively limiting the hydrogel's ability to absorb and retain physiological saline. This argument is supported by our observation that the glycerol-containing B-series hydrogels (BG, BGS30, and BGS300), exhibited approximately twice the HC compared to their counterparts in the A-series. Since the concentration of glycerol was kept constant in both the A and B-series, with only variations in agarose and sucrose concentrations, it is plausible to suggest that bonding interactions between glycerol and water might have been higher in the B-series in comparison to the A-series, and the plasticizing effect of glycerol on the B-series hydrogels might have been comparatively less pronounced than that of the A-series. Contrarily, the addition of sucrose alone in the agarose hydrogels did not exert a statistically significant impact on the HC of the hydrogels. Hence, as reported for the surface wettability of the hydrogels, glycerol has a predominant influence on the hydration capacity of the hydrogels compared to sucrose.

3.3. Dynamic Viscoelasticity

The storage (G') and loss (G'') modulus of the hydrogels were determined across a frequency range from 30.00 to 0.01 Hz under constant amplitude and compression deformation conditions. As shown in Figure 3a, the hydrogels of the A-series exhibited relatively stable behavior even at low frequencies, indicating that their bulk structure and mechanical properties were maintained within this frequency range. With the B-series, G' and G'' (Figure S5a, Supporting Information) were much more unstable compared to the A-series. This behavior was consistent irrespective of addition of sucrose or glycerol. However, the reason for this behaviour remains unclear.

The hydrogels of the A-series displayed viscoelastic behavior, with a predominant elastic component over the viscous component ($G' \gg G''$). This observation suggests a high degree of crosslinking of the agarose polymer within the hydrogels. Notably, all the hydrogels exhibited strain-stiffening behavior, with a gradual increase in G' and G'' from 9.5 to 30.0 Hz. This transition from the linear viscoelastic region to a more elastic region is typical of agarose hydrogels,^[60] attributed to their semi-flexible and geometrically connected fibrils with persistence length approximately equal to their contour length.^[61] Sucrose and glycerol had minimal impact on G' and G'' , as evidenced by the overlapping curves of native agarose hydrogels and agarose hydrogels containing either sucrose, glycerol, or their combination.

The G' values of the A-series hydrogels were examined at 9.5 Hz, considered as the end of the LVR. Figure 3b shows that the G' values ranged from 10.7 to 13.7 kPa, but the differences were marginal. Only AG and AS₃₀₀ were significantly different from A1, indicating that while glycerol slightly reduced the stiffness of the hydrogels, the addition of sucrose enhanced stiffness,

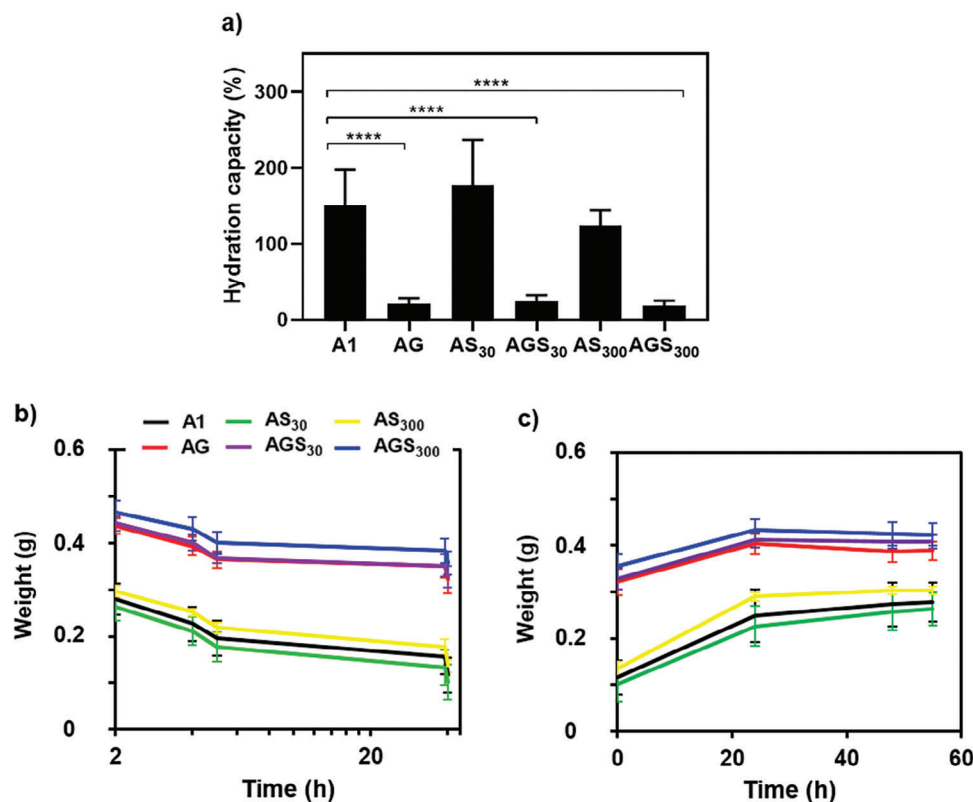


Figure 2. Hydration capacity of the series A of hydrogels in NaCl solution (0.9% w/v): a) HC values as calculated with Equation 1 (presented as mean \pm SD, $n \geq 5$); b,c) Weight evolution of the hydrogels measured during (b) dehydration at 37 °C and (c) rehydration at room temperature (presented as mean \pm SD, $n \geq 5$).

albeit at a sufficient concentration since AS₃₀ did not differ significantly from A1. Similarly, sucrose increased G'' as shown in Figure 3c. Notably, only hydrogels containing sucrose or its combination with glycerol differed significantly from A1. In the case of the B-series, the instability of G' and G'' prevents any conclusion about the difference between hydrogels, except that G' are significantly higher compared to the A-series (Figure 3b). This was not surprising given the expected influence of agarose (twice more concentrated in the B-series than in the A-series) on the stiffness of the hydrogel.^[62]

Though not statistically significant, the reduction in G' by glycerol for the A-series was not surprising, given that glycerol is a known plasticizer that enhances the flexibility of hydrogels.^[63] However, currently, there are no reports which specifically investigated the influence of glycerol on the mechanical properties of agarose hydrogels. The marginal increase in stiffness by sucrose may be attributed to enhanced hydrogen bonding with agarose polymer chains, strengthening the hydrogel network. This view was also considered by Chen et al.^[64] who examined the influence of sugar concentration on the mechanical properties of a zwitterionic polymer hydrogel. Another proposition is that sucrose acts as a filler within the hydrogel matrix, increasing the packing density of polymer chains and thus stiffening the network. Furthermore, the combined effect of sucrose and glycerol on both G' and G'' looked like the effect of sucrose alone, suggesting that the binding affinity of sucrose with the polymer matrix was predominant in comparison with the plasticizing effect of glycerol.

3.4. Surface Chemistry

The Raman spectra of sucrose and glycerol of the hydrogel matrix of the A-series, specifically at the surface and a depth of 500 μm , are depicted in Figure 4. The spectra exhibited bands characteristics for sucrose, with notable but weak signals both within (500 μm depth) and at the hydrogel surface, probably due to the relatively low concentration of sucrose.^[65] We discerned minor peaks around 1459 and 1123 cm^{-1} , associated with the scissoring vibration of CH_2 and the stretching deformation of C-OH, respectively.^[47,65] Notably, these peaks were more pronounced in the AS₃₀₀ sample compared to AS₃₀. Interestingly, these peaks vanished within the hydrogel and the 1123 cm^{-1} peak red shifted to 1139 cm^{-1} . This suggests probable weak intermolecular bonds due to chemical or physicochemical bonds. In addition to these observations, characteristic peaks of sucrose were observed around 1056 and 998 cm^{-1} , corresponding to the stretching of C-O in the furanoid ring and C-C in the glucose moiety, respectively.^[66] Remarkably, while these peaks exhibited greater prominence at the surface of AS₃₀₀ compared to AS₃₀, the reverse pattern was noted within the hydrogel, possibly due to interactions with dangling polymer chains present in the bulk of the hydrogel, which were not physically crosslinked.

On the other hand, the glycerol bands exhibited higher intensity at the hydrogel surface than, potentially indicating a concentration gradient of glycerol between the surface and in the bulk of the hydrogel. An intense doublet peak was present at 1107 and

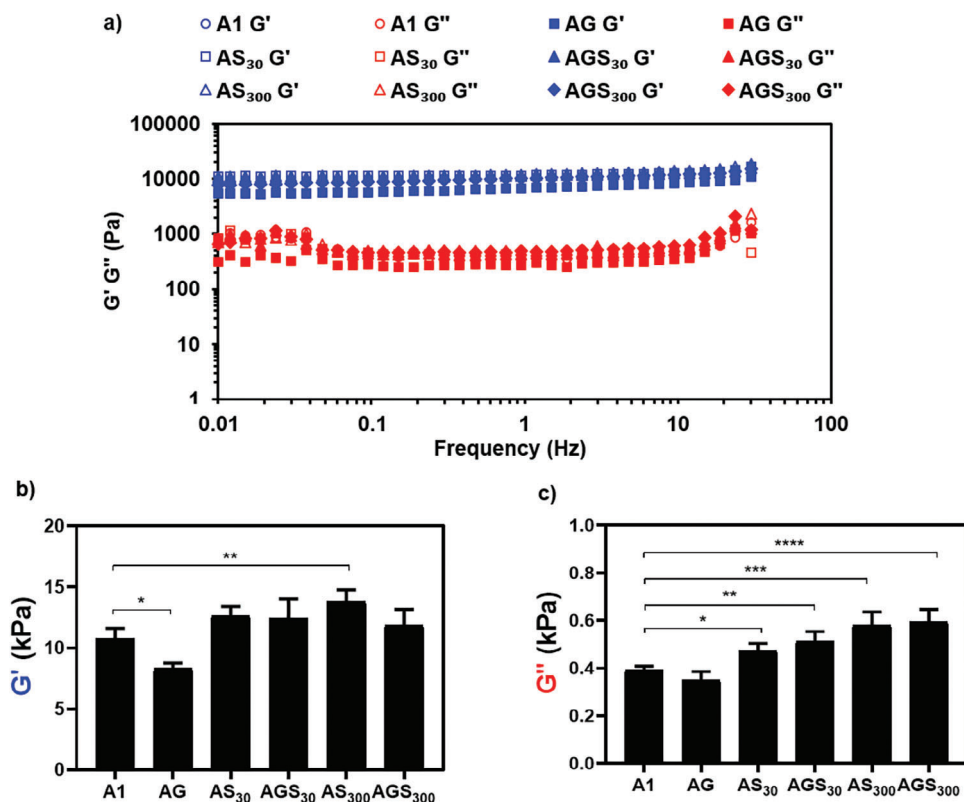


Figure 3. Viscoelastic properties of the series A of hydrogels: a) Dependence of the storage modulus (G') and loss modulus (G'') of the hydrogels on frequency (30 to 0.01 Hz) at applied stress of 0.2 to 0.3%; b) Storage (G') and c) loss (G'') modulus of the hydrogels at 9.5 Hz (values presented as mean \pm SD, $n = 3$).

1054 cm^{-1} and this corresponds to the stretching vibration of C-OH in glycerol.^[67] Additionally, peaks at 976 and 921 cm^{-1} were identified, which were associated with the rocking of CH_2 .^[68] Medium-intensity peaks at 850 and 547 cm^{-1} were also observed, corresponding to the C-C stretching and C-C-C deformation, respectively in glycerol.^[68] Finally, especially at the surface, glycerol manifested a prominent peak around 1464 cm^{-1} , alongside broad peaks at 1310 and 1254 cm^{-1} , linked to the twisting of CH_2 .^[67] Interestingly, the addition of sucrose led to a noteworthy modulation of the intensity of this peak at the surface, with the AGS₃₀₀ sample exhibiting an intensity over four times lower than AGS₃₀, along with a slight rightward shift. This reduction in the intensity of the glycerol Raman peak at 1464 cm^{-1} with increased sucrose concentration is likely attributable to alterations in the surface viscosity of the hydrogel, which can skew the Raman signal, as suggested by Itoh and Bell.^[69] Furthermore, the increased concentration of sucrose may have impacted the hydrogen bonding environment of glycerol. Indeed, sucrose is known to form hydrogen bonds with water molecules^[70] and the vibration of the CH_2 group in glycerol is sensitive to the hydrogen bonding environment, in particular to water molecules.^[70] As sucrose concentration increases, the number of hydrogen bonds between sucrose and water molecules also increases, potentially disrupting the hydrogen bonding network within glycerol-water clusters and resulting in a reduction in the intensity of the Raman peak at 1464 cm^{-1} .^[71] Intriguingly, this effect of increasing sucrose concentration on the peak intensity was not as pronounced within

the hydrogel, likely due to the higher concentration of water molecules present inside the hydrogel compared to its surface.^[68] Combining glycerol with sucrose thus had an evident impact on the glycerol peaks.

3.5. Sucrose and Glycerol Release in Water

The quantity of sucrose and glycerol released from hydrogels upon immersion in water was estimated by analyzing the ATR-FTIR spectra of the supernatants and the results are presented in Figure 5. These estimations were based on the calibration curves (Figure S1a,b) previously established for sucrose and glycerol in water. The peaks at 1044 cm^{-1} for glycerol and 1056 cm^{-1} for sucrose were selected due to the intense characteristic spectral bands of these compounds within the fingerprint region (900–1400 cm^{-1}) of the mid-infrared spectral range.^[72] However, quantification based on the 998 cm^{-1} or 1138 cm^{-1} peak with the associated calibration curves resulted in similar estimations (data not shown).

The quantities of sucrose and glycerol released are presented in Table 3. Notably, it was not possible to estimate the quantity of sucrose released from AS₃₀ due to a relatively flat spectral band, especially within the fingerprint region. This observation could be attributed to several factors, including the possibility that either no sucrose was released, or the amount of released sucrose was below the ATR method's detection limit.^[73] However, the

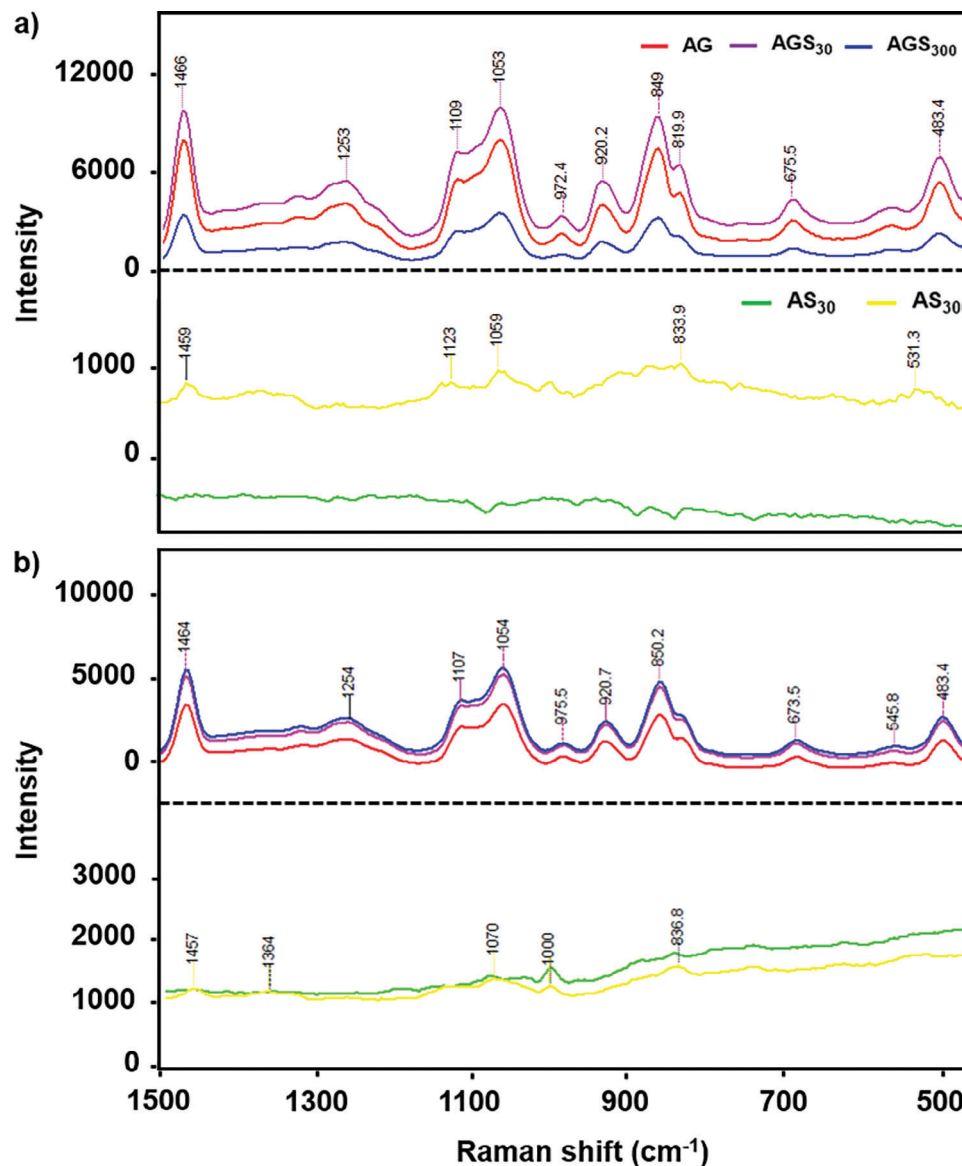


Figure 4. Raman spectra acquired a) at the surface and b) at 500 μm depth of the A-series hydrogels.

latter appears to be the most plausible explanation, as increasing the sucrose concentration, as observed in AS₃₀₀, led to a slightly more prominent band and a broad peak at 1056 cm^{-1} , indicating approximately 0.45% (w/v) of sucrose released. When combined with glycerol, it was also not possible to estimate the quantity of sucrose released from both AGS₃₀₀ and AGS₃₀ due to the low intensity of the sucrose peak at 1056 cm^{-1} .

3.6. Bacterial Growth Inhibition

Log CFU mL^{-1} (Figure 6 and Figure S6a,b, Supporting Information) of the respective test bacteria, in planktonic state, was used as an index to measure their growth inhibition by the hydrogels. Similar patterns were observed for A-series and B-series. Firstly, we observed that hydrogels containing glycerol (AG) and sucrose

(AS₃₀ and AS₃₀₀) had similar effects on *S. epidermidis* than A1. While this result was expected for AS₃₀ and AS₃₀₀ due to the very low quantity of sucrose released from the hydrogels, it was unexpected in the case of AG because glycerol is commonly used as an osmotic agent in food preservation.^[74,75] Osmotic agents typically reduce the water activity (Aw) of the substrate, leading to osmotic stress, plasmolysis, and impaired growth or lysis of microorganisms.^[76,77] It is a general notion that bacteria require a minimum Aw of 0.91 for growth.^[78] Hence lowering the Aw will consequently impede their growth. We can thus hypothesize that the amount of glycerol released from the hydrogels may not have been sufficient to critically lower the Aw, induce osmotic stress, and finally inhibit the growth of *S. epidermidis*.

In contrast, though desirable, we found that glycerol inhibited the growth of *P. aeruginosa* by 28%, as illustrated in Figure 6b. The inhibitory effect of glycerol can be attributed to a reduction

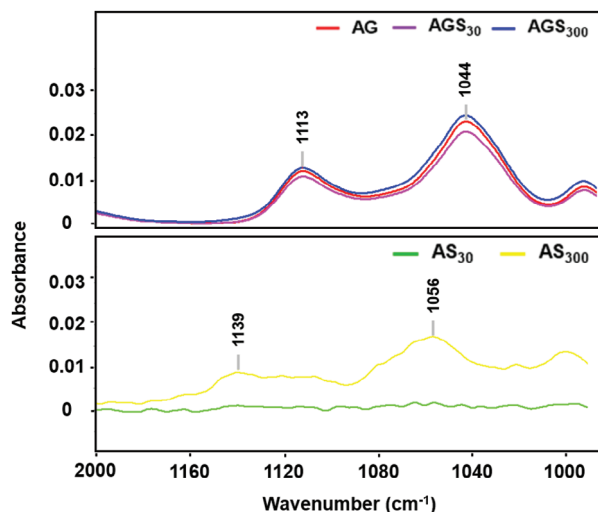


Figure 5. ATR spectra (1200–1000 cm^{-1} zoom) of sucrose and glycerol released from the hydrogels after immersion in water for 24 h.

Table 3. Quantity of sucrose and glycerol released in water as estimated from the FTIR-ATR spectra.

Samples	Sucrose [% weight/volume]	Glycerol [% weight/volume]
AG	na	8.43
AS ₃₀	na	Na
AGS ₃₀	nd	7.60
AS ₃₀₀	0.45	Na
AGS ₃₀₀	nd	8.93

nd, not determined; na, not applicable.

in the Aw of the medium.^[45] On another hand, glycerol can penetrate bacterial cells by facilitated diffusion thereby increasing intracellular osmotic pressure, weakening the membrane, and consequently inducing cellular lysis.^[79] However, this finding diverges from the results reported by Scofield et al.^[80] who indicated that glycerol promotes the growth of *P. aeruginosa* by serving as a nutrient source. The discrepancy between their findings and ours may be attributed to differences in glycerol concentration and experimental conditions employed in our respective studies. Besides, the increased susceptibility of *P. aeruginosa*

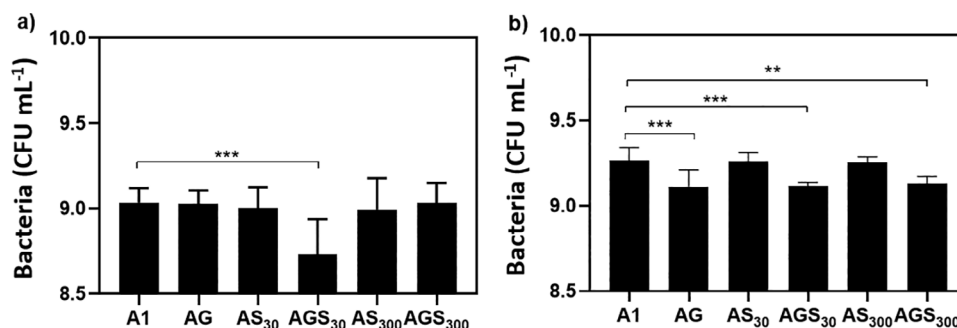


Figure 6. Antibacterial activity of the A-series hydrogels against a) *S. epidermidis* 35984 and b) *P. aeruginosa* ATCC 27853 (values presented as mean \pm SD, $n \geq 6$).

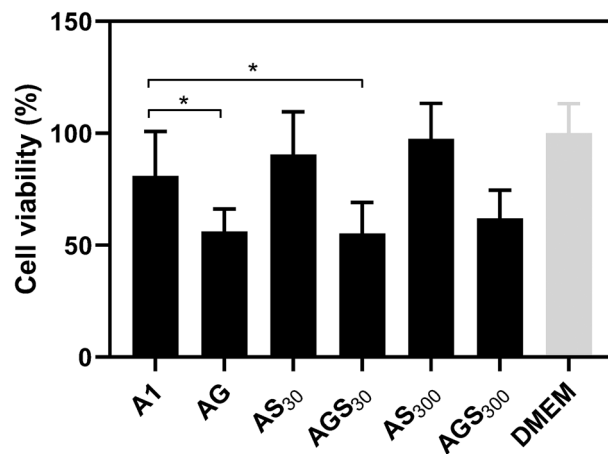


Figure 7. Cytotoxicity of the A-series hydrogel extracts on NIH/3T3 murine fibroblasts (values presented as mean \pm SD, $n = 12$).

to glycerol, compared to *S. epidermidis* could be explained by the difference in the thickness of their peptidoglycan layers. Specifically, *P. aeruginosa* has a thinner peptidoglycan layer, constituting only 10% of its cell wall, while *S. epidermidis* has a significantly thicker peptidoglycan layer, composing 90% of its cell wall.^[79]

Both AGS₃₀ and AGS₃₀₀ significantly inhibited the growth of *P. aeruginosa* by 29 and 26%, respectively. This level of inhibition was consistent with that observed with AG thus strongly suggesting that the inhibitory effect on *P. aeruginosa* may be principally due to the glycerol. More interestingly, although sucrose and glycerol individually had no inhibitory effect on the growth of *S. epidermidis*, the combination of both compounds in AGS₃₀ significantly ($p \leq 0.001$) inhibited its growth by 63% relative to A1. This synergistic inhibitory effect of sucrose and glycerol on *S. epidermidis* was only evident with the lowest sucrose concentration, as no growth inhibition was observed with AGS₃₀₀.

3.7. In Vitro Cytotoxicity

The cytotoxicity of the hydrogels was assessed by measuring the metabolic activity of NIH/3T3 murine fibroblasts exposed to hydrogel extracts in DMEM. A cytotoxic effect was defined as a reduction in cell viability greater than 30%.^[81] Figure 7 shows that the viability of fibroblasts exposed to A1, AS₃₀, and AS₃₀₀ extracts

exceeded the 70% threshold, with 81, 90, and 98% viability respectively. The increase in viability measured with the hydrogels containing sucrose suggests that sucrose positively influenced fibroblast viability in a subtle dose-dependent manner. A similar and even more pronounced trend was observed with the B-series hydrogels (Figure S7, Supporting Information), where fibroblast viability for BS₃₀ and BS₃₀₀ reached 96% and 111%, respectively. The non-toxicity of sucrose towards fibroblasts was expected, as sucrose is a preferred carbon source for both eukaryotic and prokaryotic cells.^[82]

In contrast to AS₃₀ and AS₃₀₀, AG, AGS₃₀, and AGS₃₀₀ were relatively cytotoxic as the viability of fibroblasts in their respective extracts was 56%, 55%, and 62%, respectively. The cytotoxic effect was attributed to glycerol, which was the common component in these hydrogels. This finding deviates from that of Barros et al.^[83] who suggested that glycerol was non-toxic to fibroblasts and keratinocytes. It was also unexpected given the widespread use of glycerol as a pharmacopeia compound in the food, pharmaceutical, and cosmetics industries for manufacturing various personal care and consumable products.^[84] However, by simply doubling the concentration of sucrose, as in the case of BGS₃₀ and BGS₃₀₀ (Figure S7, Supporting Information), the viability of fibroblasts recorded 74.3% and 83% respectively. This observation gives credence to our position on the cytotoxicity of glycerol to the fibroblasts, and shows that sucrose, which promoted fibroblast viability, can counteract this toxicity.

Finally, this study explored the effects of sucrose and glycerol on the viscoelasticity, HC, surface wettability, in vitro toxicity against NIH/3T3 fibroblasts, and bacteriostatic activity of AHs, contributing to the ongoing efforts to develop hydrogels with improved or tunable mechanical, physicochemical, and antibacterial properties, and reduced cytotoxicity. Our findings revealed that, interestingly, sucrose, at the lowest sucrose concentration, in combination with glycerol synergistically inhibited the growth of *S. epidermidis*, which differs from the effect of sucrose alone and from the inhibition of the growth of *P. aeruginosa*, irrespective of the concentration of sucrose. The sucrose-glycerol combination also significantly mitigated the toxic impact of glycerol on fibroblast cells, but in a dose-dependent manner. However, it did not counteract the anti-hydration effect induced by glycerol. In terms of mechanical properties, the combination of sucrose and glycerol had a negligible effect compared to the impact of sucrose alone but differed from the effect of glycerol alone. Thus, the addition of sucrose or glycerol in AHs allows to tune hydration, an essential characteristic of hydrogels in their utility in varied biomedical applications, and even holds promise for enhancing the antibacterial properties of AHs if they are combined.

4. Conclusions and Prospects

In this study, we synthesized a series of AHs using glycerol and varied concentrations of sucrose as additives. The effects of these additives on the physicochemical, biological, and mechanical properties of the hydrogels were investigated. While sucrose had negligible effects on surface wettability, HC, and viscoelasticity and bacteriostatic activity of the hydrogels, it enhanced the viability of fibroblasts. On the other hand, glycerol significantly reduced both HC and viscoelasticity of the hydrogels, while mildly inhibiting the growth of *P. aeruginosa* and the viability of fibro-

blasts. Finding a balance between bacteriostatic activity and biocompatibility is crucial. One strategy to achieve this balance could be to optimize the concentrations of both sucrose and glycerol in the hydrogels. Also, a supplementary additive, for instance an antibiotic, can be incorporated to augment the activities of sucrose and glycerol. Although the hydrogels synthesized in this study exhibited modest antibacterial activities, they are a viable alternative to hydrogels synthesized with high concentrations of antibiotics, which are often cytotoxic. This approach can potentially enhance the biocompatibility of the antibacterial hydrogel, making it a safer option for various biomedical applications. We envisage that our agarose-based hydrogels can potentially be used as materials for wound dressing and coatings for medical devices, and to formulate bioinks for 3D bioprinting. They can also be used as scaffolds for promoting cell growth and differentiation while concurrently minimizing the risk of infections.

Supporting Information

Supporting Information is available from the Wiley Online Library or from the author.

Acknowledgements

The authors would like to thank Payzulaeva Khava and Zülal Uğur for their contribution in the preliminary synthesis and characterization of the hydrogels.

Conflict of Interest

The authors declare no conflict of interest.

Author Contributions

V.C.I.: methodology, formal analysis (hydrogel synthesis and characterization), visualization, writing—original draft, review and editing; V.B.: investigation and formal analysis (rheology), writing—review; N.B.: investigation and formal analysis (rheology, microbiology, surface wettability, hydration capacity); S.G.: formal analysis (ATR-FTIR and Raman), writing—review; S.H.: investigation, supervision, and formal analysis (microbiology), writing—review; J.S.: conceptualization, formal analysis (hydrogel synthesis and characterization); C.N.: conceptualization, project administration, resources, supervision, validation, methodology, writing—original draft, review, and editing; L.P.: conceptualization, project administration, resources, supervision, validation, methodology, formal analysis (microbiology), visualization, writing—original draft, review, and editing. All authors have read and agreed to the published version of the manuscript.

Data Availability Statement

The data that support the findings of this study are available from the corresponding author upon reasonable request.

Keywords

agarose, bacteriostatic, glycerol, hydrogel, sucrose

Received: April 23, 2024
Revised: May 16, 2024
Published online:

- [1] A. Herrmann, R. Haag, U. Schedler, *Adv. Healthcare Mater.* **2021**, *10*, 2100062.
- [2] S. Jacob, A. B. Nair, J. Shah, N. Sreeharsha, S. Gupta, P. Shinu, *Pharmaceutics* **2021**, *13*, 357.
- [3] W. Shi, R. He, Y. Liu, *Eur. J. Biomed. Res.* **2015**, *1*, 3.
- [4] Y. Zhao, S. Song, X. Ren, J. Zhang, Q. Lin, Y. Zhao, *Chem. Rev.* **2022**, *122*, 5604.
- [5] Y. Luo, L. Cui, L. Zou, Y. Zhao, L. Chen, Y. Guan, Y. Zhang, *Carbohydr. Polym.* **2022**, *294*, 119774.
- [6] L. Peng, L. Chang, M. Si, J. Lin, Y. Wei, S. Wang, H. Liu, B. Han, L. Jiang, *ACS Appl. Mater. Ampmathsemicolon Interfaces* **2020**, *12*, 9718.
- [7] Z. Ahmad, S. Salman, S. A. Khan, A. Amin, Z. U. Rahman, Y. O. Al-Ghamdi, K. Akhtar, E. M. Bakhsh, S. B. Khan, *Gels* **2022**, *8*, 167.
- [8] D. A. Gyles, L. D. Castro, J. O. C. Silva, R. M. Ribeiro-Costa, *Eur. Polym. J.* **2017**, *88*, 373.
- [9] U. S. K. Madduma-Bandarage, S. V. Madihally, *J. Appl. Polym. Sci.* **2020**, *138*, <https://doi.org/10.1002/app.50376>.
- [10] F. Jiang, X.-W. Xu, F.-Q. Chen, H.-F. Wang, J. Chen, Y. Ru, Q. Xiao, A.-F. Xiao, *Mar Drugs* **2023**, *21*, 299.
- [11] B. L. Roach, A. B. Nover, G. A. Ateshian, C. T. Hung, **2016**.
- [12] P. Zarrintaj, S. Manouchehri, Z. Ahmadi, M. R. Saeb, A. M. Urbanska, D. L. Kaplan, M. Mozafari, *Carbohydr. Polym.* **2018**, *187*, 66.
- [13] Q. Han, A. Wang, W. Song, M. Zhang, S. Wang, P. Ren, L. Hao, J. Yin, S. Bai, *ACS Appl Bio Mater* **2021**, *4*, 6148.
- [14] J. J. Roberts, P. J. Martens, in *Biosynthetic Polym. Med. Appl.*, Elsevier, xx xx **2016**, pp. 205.
- [15] V. Subramanian, D. Varade, in *Biopolym. Compos. Electron.*, Elsevier, xx xx **2017**, pp. 155.
- [16] Y. Ko, J. Kim, H. Y. Jeong, G. Kwon, D. Kim, M. Ku, J. Yang, Y. Yamauchi, H.-Y. Kim, C. Lee, J. You, *Carbohydr. Polym.* **2019**, *203*, 26.
- [17] Q. Bai, C. Zheng, W. Chen, N. Sun, Q. Gao, J. Liu, F. Hu, S. Pimpi, X. Yan, Y. Zhang, T. Lu, *Mater. Adv.* **2022**, *3*, 6707.
- [18] J. G. Heuko, M. E. R. Duarte, A. G. Gonçalves, M. D. Nosedá, F. S. Murakami, M. M. de Carvalho, D. R. B. Ducatti, *Carbohydr. Res.* **2021**, *507*, 108387.
- [19] W. Gong, R. Wang, H. Huang, Y. Hou, X. Wang, W. He, X. Gong, J. Hu, *Int. J. Biol. Macromol.* **2023**, *227*, 698.
- [20] J. M. Grolman, M. Singh, D. J. Mooney, E. Eriksson, K. Nuutila, *J. Burn Care Ampmathsemicolon Res.* **2019**, *40*, 900.
- [21] I. P. Khosalim, Y. Y. Zhang, C. K. Y. Yiu, H. M. Wong, *Sci. Rep.* **2022**, *12*, 1971.
- [22] S. Liu, X. Liu, Y. Ren, P. Wang, Y. Pu, R. Yang, X. Wang, X. Tan, Z. Ye, V. Maurizot, B. Chi, *ACS Appl. Mater. Interfaces* **2020**, *12*, 27876.
- [23] N. Ninan, A. Forget, V. P. Shastri, N. H. Voelcker, A. Blencowe, *ACS Appl. Mater. Ampmathsemicolon Interfaces* **2016**, *8*, 28511.
- [24] R. Carpa, A. Remizovschi, C. A. Culda, A. L. Butiuc-Keul, *Gels* **2022**, *8*, 70.
- [25] B. Hu, C. Owh, P. L. Chee, W. R. Leow, X. Liu, Y.-L. Wu, P. Guo, X. J. Loh, X. Chen, *Chem. Soc. Rev.* **2018**, *47*, 6917.
- [26] Y. Zhong, H. Xiao, F. Seidi, Y. Jin, *Biomacromolecules* **2020**, *21*, 2983.
- [27] S.-H. Chen, Z. Li, Z.-L. Liu, L. Cheng, X.-L. Tong, F.-Y. Dai, *J. Mater. Res.* **2019**, *34*, 1911.
- [28] Z. Yang, R. Huang, B. Zheng, W. Guo, C. Li, W. He, Y. Wei, Y. Du, H. Wang, D. Wu, H. Wang, *Adv. Sci.* **2021**, *8*, 2003627.
- [29] S. Hamidi, F. Monajjemzadeh, M. Siahi-Shadbad, S. A. Khatibi, A. Farjami, *Polym. Eng. Ampmathsemicolon Sci.* **2022**, *63*, 5.
- [30] M. A. Cook, G. D. Wright, *Sci. Transl. Med.* **2022**, *14*, eabo7793.
- [31] V. N. J. Lekahena, M. R. Boboleha, in *Proc. 5th Int. Conf. Food Agric. Nat. Resour. FANRes* **2019**, Atlantis Press, 2020.
- [32] P. M. Schlievert, M. L. Peterson, *PLoS One* **2012**, *7*, e40350.
- [33] J. R. White, *Clin. Diabetes Publ. Am. Diabetes Assoc.* **2018**, *36*, 74.
- [34] V. Normand, *Carbohydr. Polym.* **2003**, *54*, 83.
- [35] A. Biswas, M. Bharara, C. Hurst, R. Gruessner, D. Armstrong, H. Rilo, *J. Diabetes Sci Technol* **2010**, *4*, 1139.
- [36] J. A. Mora Vargas, J. O. Ortega, M. B. C. dos Santos, G. Metzker, E. Gomes, M. Boscolo, *Carbohydr. Res.* **2020**, *489*, 107957.
- [37] Y. Ning, M. Ma, Y. Zhang, D. Zhang, L. Hou, K. Yang, Y. Fu, Z. Wang, Y. Jia, *Food Res Int* **2022**, *154*, 111018.
- [38] S.-Y. Shao, Y.-G. Shi, Y. Wu, L.-Q. Bian, Y.-J. Zhu, X.-Y. Huang, Y. Pan, L.-Y. Zeng, R.-R. Zhang, *Molecules* **2018**, *23*, 1118.
- [39] S. J. Reid, V. R. Abratt, *Appl. Microbiol. Biotechnol.* **2005**, *67*, 312.
- [40] W. B. Setianto, T. Y. Wibowo, H. Yohanes, F. Illaningtyas, D. D. Anggoro, *IOP Conf. Ser. Earth Environ. Sci.* **2017**, *65*, 012046.
- [41] E. Basiak, A. Lenart, F. Debeaufort, *Polymers* **2018**, *10*, 412.
- [42] A. K. Yadav, S. V. Singh, *J. Food Sci Technol* **2014**, *51*, 1654.
- [43] A. Vigué, D. Vautier, A. Kaytoue, B. Senger, Y. Arntz, V. Ball, A. Ben Mlouka, V. Gribova, S. Hajjar-Garreau, J. Hardouin, T. Jouenne, P. Laval, L. Ploux, *J. Funct. Biomater* **2022**, *13*, 237.
- [44] C. H. Kung, P. K. Sow, B. Zahiri, W. Mérida, *Adv. Mater. Interfaces* **2019**, *6*, 1900839.
- [45] H. Nakagawa, T. Oyama, *Front Chem* **2019**, *7*, 731.
- [46] A. Gómez-Siurana, A. Marcilla, M. Beltrán, D. Berenguer, I. Martínez-Castellanos, S. Menargues, *Thermochim. Acta* **2013**, *573*, 146.
- [47] A. B. Brizuela, L. C. Bichara, E. Romano, A. Yurquina, S. Locatelli, S. A. Brandán, *Carbohydr. Res.* **2012**, *361*, 212.
- [48] A. Hauswirth, R. Köhler, L. ten Bosch, G. Avramidis, C. Gerhard, *Food* **2022**, *11*, 2786.
- [49] R. Nair, S. Venkatesh, K. A. Athmaselvi, S. Thakur, *J. Food Meas. Charact.* **2015**, *10*, 24.
- [50] in *ANSIAAMIISO 10993–52009R2014mathsemicolon Biol. Eval. Med. Devices —Part 5 Tests Vitro Cytotox*, AAMI, **2009**.
- [51] G. Apte, A. Lindenbauer, J. Schemberg, H. Rothe, T.-H. Nguyen, *ACS Omega* **2021**, *6*, 10963.
- [52] K. Sheng, X. Dong, Z. Chen, Z. Zhou, Y. Gu, J. Huang, *Appl. Surf. Sci.* **2022**, *591*, 153097.
- [53] K. Bialik-Wąs, K. Pluta, D. Malina, M. Barczewski, K. Malarz, A. Mrozek-Wilczkiewicz, *Int. J. Mol. Sci.* **2021**, *22*, 12022.
- [54] B. Xu, Y. Liu, L. Wang, X. Ge, M. Fu, P. Wang, Q. Wang, *Polymers* **2018**, *10*, 1025.
- [55] P. K. GhatyVenkataKrishna, G. A. Carri, *J. Biomol. Struct. Dyn.* **2013**, *32*, 424.
- [56] Y. Kataoka, N. Kitadai, O. Hisatomi, S. Nakashima, *Appl. Spectrosc.* **2011**, *65*, 436.
- [57] B. S. Flowers, M. S. Mittenthal, A. H. Jenkins, D. A. Wallace, J. W. Whitley, G. P. Dennis, M. Wang, C. H. Turner, V. N. Emel'yanenko, S. P. Verevkin, J. E. Bara, *ACS Sustain. Chem. Ampmathsemicolon Eng.* **2016**, *5*, 911.
- [58] Z. Y. Ben, H. Samsudin, M. F. Yhaya, *Eur. Polym. J.* **2022**, *175*, 111377.
- [59] J. Tarique, S. M. Sapuan, A. Khalina, *Sci. Rep.* **2021**, *11*, 13900.
- [60] L. Martikainen, K. Bertula, M. Turunen, O. Ikkala, *Macromolecules* **2020**, *53*, 9983.
- [61] K. Bertula, L. Martikainen, P. Munne, S. Hietala, J. Klefström, O. Ikkala, Nonappa, *ACS Macro Lett.* **2019**, *8*, 670.
- [62] D. Millar, M. Mennu, K. Upadhyay, C. Morley, P. Ifju, *Strain* **2021**, *57*, e12383.
- [63] M. Watanabe, H. Li, M. Yamamoto, J. Horinaka, Y. Tabata, A. W. Flake, *J. Biomed Mater Res B Appl Biomater* **2020**, *109*, 921.
- [64] Y. Chen, W. Wang, D. Wu, M. Nagao, D. G. Hall, T. Thundat, R. Narain, *Biomacromolecules* **2018**, *19*, 596.
- [65] L. S. Jr, L. M. Moreira, V. G. B. Conceição, H. L. Casalechi, I. S. Muñoz, F. F. D. Silva, M. A. S. R. Silva, R. A. D. Souza, M. T. T. Pacheco, *Spectroscopy* **2009**, *23*, 217.
- [66] K. Ilaslan, I. H. Boyaci, A. Topcu, *Food Control* **2015**, *48*, 56.
- [67] A. Mudalige, J. E. Pemberton, *Vib. Spectrosc.* **2007**, *45*, 27.
- [68] E. Mendelovici, R. L. Frost, T. Klopprogge, *J. Raman Spectrosc.* **2000**, *31*, 1121.
- [69] N. Itoh, S. E. J. Bell, *Analyst* **2017**, *142*, 994.
- [70] M. Yamashina, M. Akita, T. Hasegawa, S. Hayashi, M. Yoshizawa, *Sci. Adv.* **2017**, *3*, e1701126.

- [71] Y. Liu, K. Huang, Y. Zhou, D. Gou, H. Shi, *J. Phys. Chem. B* **2021**, *125*, 8099.
- [72] L. F. Leopold, N. Leopold, H.-A. Diehl, C. Socaciu, *Spectroscopy* **2011**, *26*, 93.
- [73] J.-J. Max, C. Chapados, *J. Phys. Chem. A* **2001**, *105*, 10681.
- [74] E. K. Dermesonlouoglou, M. C. Giannakourou, *J Food Sci Technol* **2018**, *55*, 4079.
- [75] K. Pattanapa, N. Therdthai, W. Chantrapornchai, W. Zhou, *Int. J. Food Sci. Ampmathsemicolon Technol.* **2010**, *45*, 1918.
- [76] L. Qiu, M. Zhang, J. Tang, B. Adhikari, P. Cao, *Food Res Int* **2019**, *116*, 90.
- [77] S. Zeidler, V. Müller, *Environ. Microbiol.* **2019**, *21*, 2212.
- [78] L. V. Allen Jr, *Int J Pharm Compd* **2018**, *22*, 288.
- [79] V. S. M. Saegeman, N. L. Ectors, D. Lismont, B. Verduyck, J. Verhaegen, *Burns* **2008**, *34*, 205.
- [80] J. Scofield, L. Silo-Suh, *Can. J. Microbiol.* **2016**, *62*, 704.
- [81] E. Jablonská, J. Kubásek, D. Vojtěch, T. Ruml, J. Lipov, *Sci. Rep.* **2021**, *11*, 6628.
- [82] T. Franzino, H. Boubakri, T. Cernava, D. Abrouk, W. Achouak, S. Reverchon, W. Nasser, F. el Z. Haichar, *Plant Commun* **2022**, *3*, 100272.
- [83] N. R. de Barros, R. S. dos Santos, M. C. R. Miranda, L. F. C. Bolognesi, F. A. Borges, J. V. Schiavon, R. F. C. Marques, R. D. Herculano, A. M. Q. Norberto, *Skin Res Technol* **2019**, *25*, 461.
- [84] S. Goyal, N. B. Hernández, E. W. Cochran, *Polym. Int.* **2021**, *70*, 911.